

IAC-STAR: A CODE FOR SYNTHETIC COLOR-MAGNITUDE DIAGRAM COMPUTATION

ANTONIO APARICIO

Departamento de Astrofísica, Universidad de La Laguna; and Instituto de Astrofísica de Canarias,
Calle Vía Láctea s/n, E-38200 La Laguna, Tenerife, Spain

AND

CARME GALLART

Instituto de Astrofísica de Canarias, Calle Vía Láctea s/n, E-38200 La Laguna, Tenerife, Spain

Received 2003 August 13; accepted 2004 May 6

ABSTRACT

The code IAC-STAR is presented. It generates synthetic H-R and color-magnitude diagrams (CMDs) and is mainly aimed at star formation history studies in nearby galaxies. Composite stellar populations are calculated on a star-by-star basis, by computing the luminosity, effective temperature, and gravity of each star by direct bilogarithmic interpolation in the metallicity and age grid of a library of stellar evolution tracks. Visual (broadband and *Hubble Space Telescope*) and infrared magnitudes are also provided for each star after applying bolometric corrections. The Padua stellar evolution libraries of Bertelli et al. and Girardi et al., respectively, and the Teramo stellar evolution library by Pietrinferni et al., as well as various bolometric corrections libraries are used in the current version. A variety of star formation rate functions, initial mass functions, and chemical enrichment laws are allowed, and binary stars can be computed. Although the main motivation of the code is the computation of synthetic CMDs, it also provides integrated masses, luminosities, and magnitudes, as well as surface brightness fluctuation luminosities and magnitudes for the total synthetic stellar population, and therefore it can also be used for population synthesis research. The code is offered for free use and can be accessed at the IAC-STAR Web site. The only requirement is that this paper be referenced and credited as indicated there.

Key words: color-magnitude diagrams — Hertzsprung-Russell diagram — stars: formation

1. INTRODUCTION

Galaxies evolve on two main paths: dynamically, including interactions and mergers with external systems, and through the process of the formation, evolution, and death of stars within them. Among the effects of the latter that concern us here are the following: (1) the evolution of gas content, (2) the chemical enrichment, and (3) the formation of the stellar populations with properties that evolve following the evolution of the gas from which they form. The star formation history (SFH) is therefore fundamental to understanding the galaxy evolution process.

The color-magnitude diagram (CMD) is the best tool to study and derive the SFH of a galaxy. Deep CMDs display stars born over the lifetime of the galaxy and are indeed fossil records of the SFH. A qualitative sketch of the stellar populations present in a galaxy can be done from a quick look at a good CMD. The presence of stars in characteristic evolutionary phases indicates that star formation took place in the system in different epochs of its history. For example, the presence of RR Lyrae stars is indicative of an old, low-metallicity stellar population; a substantial number of red giant branch (RGB) stars is associated with intermediate-age to old star formation activity; a well-developed red tail of asymptotic giant branch (AGB) stars shows that intermediate-age and young stars with relatively high metallicity are present in the system, and even a few blue, bright stars, as well as H II regions are evidence of very recent star formation activity.

A higher degree of sophistication is provided by isochrone fitting to significant features of the CMD. Indeed, this method is simple and powerful enough to determine the age and metallicity of single stellar populations such as the ones present in star clusters.

However, actually deciphering the information contained in a complex CMD and deriving a quantitative, accurate SFH is complicated and requires more sophisticated techniques. The standard procedure involves three main ingredients: (1) good data, from which a deep observational CMD can be plotted, ideally reaching the oldest main-sequence turnoffs; (2) a stellar evolution library complemented by a bolometric correction library providing colors and magnitudes of stars as a function of age, mass, and metallicity; and (3) a method to relate the number of stars populating different regions of the observational CMD with the density distribution of stars in the CMD as a function of age, mass, and metallicity as predicted by the stellar evolution theory. The result of this comparison provides the SFH of the system.

Usually, item 3 involves computation of one or several synthetic CMDs from which the star density distribution predicted from theory is deduced. Indeed, the synthetic CMD technique is the most powerful one available for this kind of analysis and, in general, for the study of the SFH of resolved stellar populations. The first to compute and use a synthetic CMD using a Monte Carlo technique was Maeder (1974). Chiosi et al. (1988) presented the first application of the Padua synthetic CMD code. Tosi et al. (1991) used, for the first time, luminosity functions derived from synthetic CMDs to sketch recent SFHs of nearby galaxies. Bertelli et al. (1992) were the first to use the global detailed morphology together with number counts and ratios of star counts in different areas of the synthetic and observed CMDs to derive the SFH of a galaxy (the LMC).

A more recent version of the Padua code is ZVAR, the distinctive feature of which is the age and metallicity interpolation. They are performed for each single star in the Padua

grid of stellar evolution tracks. This has been a heavily used code in the recent past (e.g., Gallart et al. 1996; Vallenari et al. 1996a, 1996b; Aparicio et al. 1997a, 1997b; Hurley-Keller et al. 1998; Gallart et al. 1999; Aparicio et al. 2000; Vallenari et al. 2000; Bertelli & Nasi 2001; Ng et al. 2002; Bertelli et al. 2003; see Aparicio et al. 1996 for several examples of synthetic CMDs using ZVAR and Aparicio 2002, for a review). Other codes have been developed by different groups for the computation of synthetic CMDs (see Tolstoy & Saha 1996; Dolphin 1997; Holtzman et al. 1999; Ardeberg et al. 1997; Stappers et al. 1997; Dohm-Palmer et al. 1997; Hernández et al. 1999; Harris & Zaritsky 2001).

In this paper we present a new algorithm for the computation of synthetic CMDs. It is intended to be as general as possible. For this purpose, a variety of inputs for the initial mass function (IMF), SFH, metallicity law, and binarity are allowed. Stars with age and metallicity following a continuous distribution are computed through interpolation in a stellar evolution library, providing synthetic CMDs with smooth, realistic stellar distributions. This significantly improves the accuracy of the comparison with observed CMDs as compared with methods without such interpolation. The Padua stellar evolution libraries by Bertelli et al. (1994; hereafter Bertelli94) and Girardi et al. (2000; hereafter Girardi00) and Teramo (Pietrinferni et al. 2004) stellar evolution library are used in the current version of the program, completed by the Cassisi et al. (2000) models for very low mass stars. Together with the luminosity and temperature of each star, the code provides the absolute magnitudes in Johnson-Cousins *UBVRI*, HST F218W, F336W, F439W, F450W, F555W, and F814 and infrared *JHKLL'M* filters. To this purpose the bolometric correction libraries by Lejeune et al. (1997), Castelli & Kurucz (2003), Girardi et al. (2002), and Origlia & Leitherer (2000) are used, the latter for the *HST* filter system. In summary, in the current version of the code, the user can select among three stellar evolution libraries and four bolometric correction libraries. The code includes the thermally pulsating AGB (TP-AGB) following the prescription of Marigo et al. (1996).

The code is made available for free use.¹ The present paper should be considered as the reference for the code. This paper will be complemented by several others presenting, in particular, a method based on a generic algorithm to compute the SFH from comparison of an observed and a generic synthetic CMD (Aparicio & Hidalgo 2004) and a library of population synthesis based in surface brightness fluctuations (Marín-Franch & Aparicio 2004).

This paper is organized as follows. In § 2, the fundamentals of synthetic CMD computation are given, including short descriptions of the stellar evolution and bolometric correction libraries used. In §§ 3, 4, and 5 the basic stellar evolution, the main features arising in a real CMD, and the main aspects of chemical enrichment laws are summarized. These topics are relevant for a better understanding of the computation process and the synthetic results. Section 6 is devoted to explaining how the code works, as well as some particularities including the computation of mass loss in advanced evolutionary phases. Section 7 is a short outline of the code input and output. A full commented list of input choices and a description of the output file content are available in the IAC-STAR Web site. This will be permanently updated, including any future

change in the input and output. Finally, a summary of the paper is given in § 8.

2. FUNDAMENTALS OF SYNTHETIC CMDs

The distribution of stars in a CMD depends on several aspects of the physics of stars and galaxies. Broadly speaking, the density of stars in a given region of the CMD is directly proportional to the time that stars of any mass and metallicity spend in that region during their evolution. This information is provided primarily by stellar evolution theory, on which the computation of synthetic CMDs strongly relies, complemented by bolometric corrections. However, since the fraction of stars formed with different masses vary with mass, the distribution of the stellar masses at birth, the so-called initial mass function (IMF), provides a second, important input characterizing the star density distribution on the CMD. Stars, however, are not formed at the same rate during the lifetime of a galaxy. The function accounting for the star formation rate (SFR) as a function of time is a further important input. Moreover, stars are born with the metallicity of the interstellar medium from which they form. So, the chemical enrichment law (CEL) of the system provides further fundamental information. The last important contribution to the morphology of the CMD comes from the fraction and mass ratio distribution of binary stars. Other physical properties do affect that morphology, such as the internal, differential reddening or the mass distribution (stellar population gradients, depth effects, etc.) within the system. However, these properties can be considered external to the CMD itself. In most (or even all) cases in which we are interested, they can be added to the computed synthetic CMD later.

In summary, the inputs necessary to compute a synthetic CMD are the following:

1. a stellar evolution library, covering a wide range of stellar evolutionary phases and stellar masses and metallicities. It should provide stellar luminosities, temperatures, and surface gravities as a function of mass, metallicity, and age;
2. a bolometric correction library to transform stellar luminosities, temperatures, and surface gravities to magnitudes in a given photometric system;
3. an IMF, $\phi(m)$;
4. an SFR function, $\psi(t)$;
5. a CEL, $Z(t)$;
6. a function accounting for the fraction of binary stars and for the distribution of the secondary to primary stellar mass ratio, $\beta(f, q)$.

In the following we comment on the stellar evolution and bolometric correction libraries used here and on the computation algorithm.

2.1. The Stellar Evolution Libraries

Computation of a synthetic CMD relies on a stellar evolutionary library, which should be computed using the most up-to-date physics and which is well tested against observations and complete in terms of ages, metallicities, and evolutionary phases. These three characteristics are difficult to accomplish, and indeed many of the accuracy and precision limitations of synthetic CMD-based techniques originate in this difficulty. In its current version, IAC-STAR uses the Bertelli94, Girardi00, and Teramo (Pietrinferni et al. 2004) stellar evolution libraries. These libraries are completed by the Cassisi et al. (2000) models for very low mass stars. Even

¹ The code can be executed at the IAC-STAR Web site <http://iac-star.iac.es>, with the only requirement that it be credited as indicated there.

TABLE 1
MODEL GRIDS USED IN THE CURRENT VERSION OF IAC-STAR

Parameters	Teramo	Girardi00	Bertelli94
Mass range (M_{\odot}).....	0.5–10	0.15–7	0.6–120
Z range (Z,nstep).....	0.0001–0.04 (10)	0.0–0.03 (8)	0.0004–0.05 (5)
$\alpha = 1/H_p$	1.913	1.68	1.63
Y_{\odot}, Z_{\odot}	0.2734, 0.0198	0.273, 0.019	0.282, 0.02
Overshooting.....	Canonical and $0.2H_p^a$	$0.5H_p^{a,b}$	$0.5H_p^{a,b}$
EOS.....	Irwin04	Kipp65+Gir96+MHD90	Kipp65
Radial opacity.....	OPAL96+Alex94	OPAL92+Alex94	OPAL92+Hueb77+Cox70
Nuclear reactions.....	NACRE+Kunz02	Caughlan88+Landré90+WW93	Caughlan88
Model atmosphere.....	Castelli02	Castelli97	Kurucz92+emp

^a The prescription on how overshooting is turned off as a function of mass heavily determines the morphology of the main sequence turnoff at intermediate ages. Teramo: $\lambda = (M/M_{\odot} - 0.9)/4$ for $1.1 M_{\odot} \leq M \leq 1.7 M_{\odot}$, $\lambda = 0.2H_p$ for $M \geq 1.7 M_{\odot}$, and $\lambda = 0$ for $M \leq 1.1 M_{\odot}$; Girardi00: $\lambda = M/M_{\odot} - 1.0$ for $1.0 M_{\odot} \leq M \leq 1.5 M_{\odot}$, with $\lambda = 0.5H_p$ for $M \geq 1.5 M_{\odot}$ and $\lambda = 0$ for $M \leq 1.0 M_{\odot}$; Bertelli94: $\lambda = 0.5H_p$ for $M \geq 1.6 M_{\odot}$ and $\lambda = 0.25H_p$ for $1.0 M_{\odot} \leq M \leq 1.5 M_{\odot}$.

^b The parameter describing overshooting is its extent λ across the border of the convective zone, in units of pressure scale height (H_p). This parameter, defined in Bressan et al. (1981), is not equivalent to others present in the literature; e.g., $\lambda = 0.5$ in the Padua formalism approximately corresponds to $0.25H_p$ above the convective border adopted by the Teramo group.

REFERENCES.—Teramo: Pietrinfermi et al. 2004; Girardi00: Girardi et al. 2000; Bertelli94: Bertelli et al. 1994; Irwin04: Irwin et al. 2004; OPAL96: Iglesias & Rogers 1996; Alex94: Alexander & Ferguson 1994; NACRE: Angulo et al. 1999; Kunz02: Kunz et al. 2002; Castelli02: Castelli & Kurucz 2003; Kipp65: Kippenhahn et al. 1965; Gir96: Girardi et al. 1996; MHD90: Mihalas et al. 1990; OPAL92: Rogers & Iglesias 1992; Caughlan88: Caughlan & Fowler 1988; Landré90: Landré et al. 1990; WW93: Weaver & Woosley 1993; Castelli97: Castelli et al. 1997; Hueb77: Huebner et al. 1997; Cox70: Cox & Stewart 1970a, 1970b; Kurucz92: Kurucz 1992.

though the Bertelli94 library has been basically superseded by Girardi00, we have chosen to include both libraries since many SFH studies in the past have been performed using Bertelli94, which may be chosen for comparative studies. It is our intention to include additional libraries in the future. In Table 1 the characteristics and main input physics of the three libraries are listed. Figure 1 shows several tracks from the Bertelli94 library, as well as two very low mass star models computed from Cassisi et al. (2000).

2.2. The Bolometric Correction Libraries

Comparison of synthetic and observed CMDs require transforming the former from the *theoretical* plane (the $T_{\text{eff}}-L$ plane) to the *observational* one (the color-magnitude plane). This is done by adopting a bolometric correction scale and a color-effective temperature relation. It is important to note that while the stellar evolution library is fundamental for the computation of the synthetic CMD itself, an equally reliable bolometric correction library is required if synthetic CMDs are to be compared with observed ones. This also implies that the derivation of accurate SFHs relies on the accuracy of both the stellar evolution library and the model atmospheres set adopted for computing the bolometric correction scale and color- T_{eff} relation.

In its current version, IAC-STAR implements four choices for the bolometric correction and color- T_{eff} relation libraries:

1. the Girardi et al. (2002) library providing bolometric corrections for visual, broadband *UBVRI*, and infrared *JHK* filters;
2. the Castelli & Kurucz (2003) library for visual, broadband *UBVRI*, and infrared *JHKL* filters, completed with the Fluks et al. (1994) semiempirical transformations for M giants. Care has been taken that the two sets properly match;
3. the Lejeune et al. (1997) library for visual, broadband *UBVRI* filters, and infrared *JHKLL'M* filters;
4. the Origlia & Leitherer (2000) library for F218W, F336W, F439W, F450W, F555W, and F814W filters of the *HST* WFPC2 and ACS.

These libraries fulfill the requirements of completeness and wide metallicity ($[Fe/H]$), temperature (T_{eff}), and gravity (g) coverage and sampling, as well as having been empirically calibrated. It is our intention to include other libraries, as well as transformations for additional photometric bands such as the Stromgren ones, as they become available in the future.

The bolometric correction and the color- T_{eff} relation are functions of these three parameters: $BC([Fe/H], T_{\text{eff}}, g)$. The libraries used allow us to obtain bolometric corrections for almost all cases, although they fail to fully cover a few, very low temperature objects. Linear extrapolation is used in such cases. Since it is rarely necessary, the deviation effects that could arise in the CMD from that extrapolation should be negligible. However, detailed analysis of color distribution of stars in phases as the extended AGB should be made with caution.

2.3. Computing a Synthetic CMD

IAC-STAR uses a Monte Carlo method to compute synthetic CMDs on a star-by-star basis. A random number generator (RNG) is used to compute first the mass and then the time of birth of the star according to the distribution functions $\phi(m)$ and $\psi(t)$, respectively. The value of time is introduced in the function $Z(t)$ to obtain the metallicity. If metallicity dispersion is allowed, its exact value is obtained using such a dispersion and a new random number. The binarity of the star is determined in a similar way, using a RNG and the function $\beta(f, q)$, in which f is the fraction of binaries and q the internal mass rate. If the object turns out to be a binary, the computed star is assumed to be the primary (most massive) star of the system. The age and metallicity of the secondary are assumed to be the same as for the primary. The mass of the secondary is computed, again using the RNG and according to the secondary-to-primary mass ratio distribution provided by q and an assumed IMF for the secondaries. The lifetime of each star according to the stellar evolution models is used at this point to decide whether the star is alive (and then to calculate its remaining parameters) or dead (and then to calculate the properties of the remnant). The case in which only the secondary star is alive is allowed.

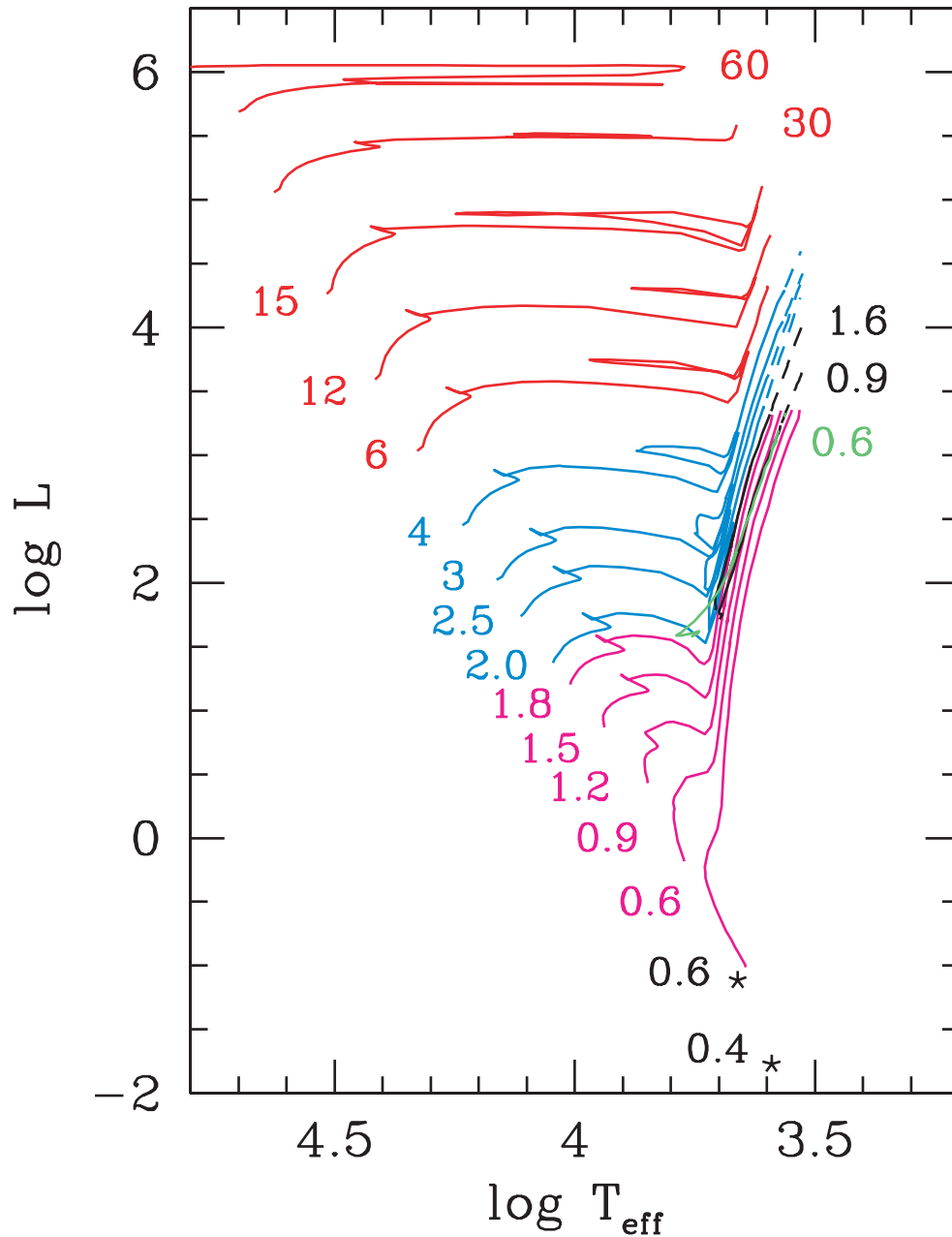


FIG. 1.—Set of evolutionary tracks for metallicity $Z = 0.004$ from the library of Bertelli94 (solid and dashed lines) extended by two very low mass models interpolated from Cassisi et al. (2000) of age 10 Gyr (stars). Colors indicate different mass ranges, as follows. Red: high-mass tracks; blue: intermediate-mass tracks; magenta: low-mass stars up to the He flash; black and green: low-mass stars on the horizontal branch. In all the cases, dashed lines represent the TP-AGB extensions of the Padua tracks computed by IAC-STAR. Labels correspond to the track initial masses, in solar masses.

Once the mass, age, and metallicity are known, the luminosity, temperature, and surface gravity of the star are computed through interpolation within the chosen stellar evolutionary library. If the star is a binary, the process is repeated for each component. Finally, luminosity, temperature, and gravity are interpolated in the chosen bolometric correction library to obtain magnitudes and colors in the standard photometric system.

These are the computation fundamentals. In § 7, we provide details about the procedure itself. But before doing so, it is helpful to outline the aspects of the stellar evolution relevant to the morphology of the CMD (§ 3), to review such morphology (§ 4), and to discuss the CEL, its parameteriza-

tion, and its relation to basic physical properties of the system (§ 5).

3. BASIC STELLAR EVOLUTION

Luminosity L and temperature T_{eff} , as a function of stellar age and metallicity, as well as lifetime, are, for our purposes, the main information provided by the stellar evolutionary library. If s is a star of mass m_s , metallicity Z_s , and age a_s , a first estimate of its location in the CMD might be obtained just by time interpolation within a single evolutionary track of age and metallicity closest to the stellar values. However, if a realistic synthetic CMD is to be computed, interpolation must be done between tracks both in age and metallicity. The fact

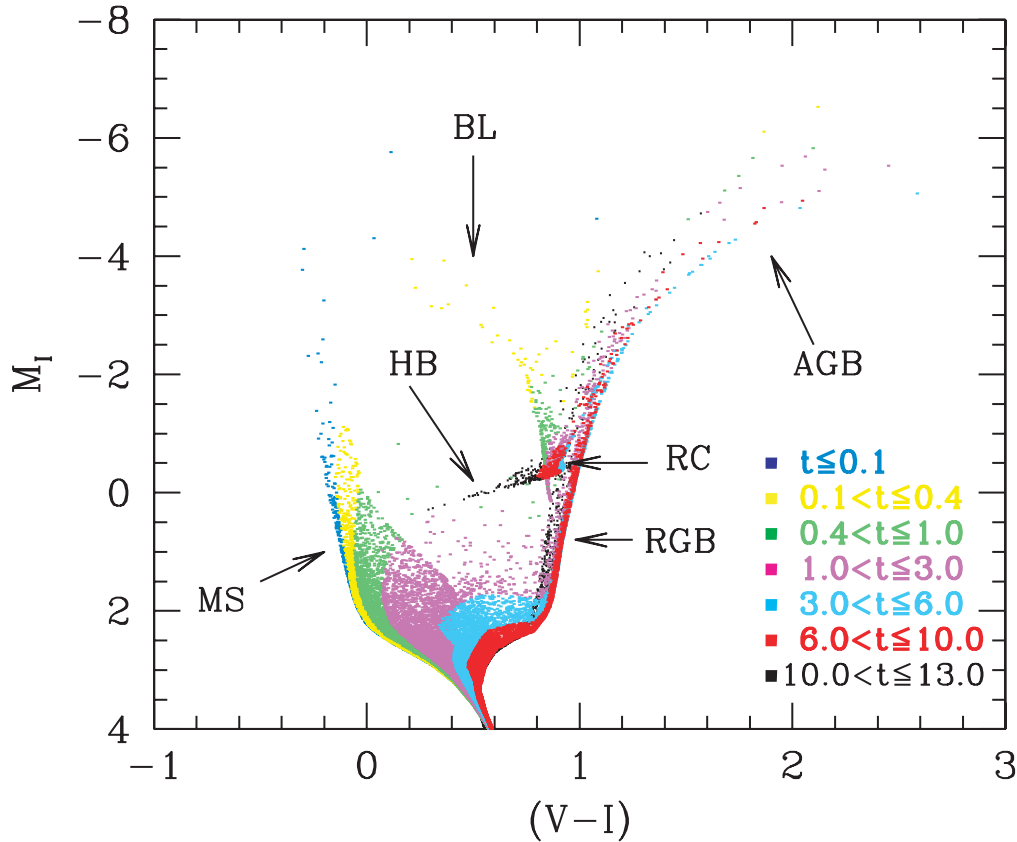


FIG. 2.—Synthetic CMD computed using constant SFR from 13 Gyr ago to date and metallicity linearly increasing from $Z_0 = 0.0001$ to $Z_f = 0.02$ and a Kroupa et al. (1993) IMF. The Bertelli94 stellar evolution library and the Lejeune et al. (1997) bolometric correction library have been used. Stars in different age intervals are plotted in different colors. The color code is given in the figure, in gigayears. Labels indicate the evolutionary phase (see text for an explanation).

that stars experience different particular physical processes along their evolution that, like the He flash, abruptly interrupt their smooth evolutionary paths, makes this interpolation rather cumbersome. In the following, we sketch the basic stellar evolution directly affecting the synthetic CMD computation problem. In this sense, it is useful to divide stars in three groups according to their masses: low-, intermediate-, and high-mass stars (see Chiosi et al. 1992 and Chiosi 1998 for a short but clear summary of the basic stellar evolution). The critical masses separating these groups depend on the chemical composition and the input physics. However, roughly, the mass separating the low and intermediate dominions, m_{lw} , is in the range $1.7\text{--}2.0 M_\odot$, and the mass separating the intermediate and high dominions, m_{up} , is in the range $5\text{--}7 M_\odot$. In Figure 2 the loci of the different features that will be introduced in the following are displayed.

Stars of any mass spend a major fraction of their lives in the core H-burning, main-sequence (MS) phase. As H is exhausted in the core, the star leaves the MS, while the H burning proceeds in a shell. At this point, a star may follow two types of paths in the CMD, depending on its mass. In low-mass stars, the H-exhausted, He core is not massive, hot, and dense enough to immediately start the He burning. The core gravitationally contracts, and as a consequence degeneracy appears in the electronic gas. This degeneracy stops the core collapse. As H burning proceeds in a shell, the star climbs the RGB and more He is incorporated into the degenerated core. When the mass of this core reaches about $0.45\text{--}0.50 M_\odot$ (the precise mass depends on chemical composition, stellar mass, and input physics), He burning starts violently, removing the

electron degeneracy. This is the so-called He flash. The star abruptly terminates the RGB phase and enters the horizontal branch, in which He burning and H burning proceed in the core and a shell, respectively. Since the He flash is produced at essentially identical core mass, the maximum RGB luminosity is almost constant, independently of the stellar metallicity and initial mass. The same happens to the luminosity of the horizontal branch (HB). However, the stellar surface effective temperature, which determines the position of the star in the HB, depends strongly on several factors, among which the most important are chemical composition and total stellar mass. It must be noted that the latter depends not only on the initial stellar mass, but also on the mass loss during the RGB and the He flash.

In intermediate- and high-mass stars, the He core ignites in nondegenerate conditions as soon as the central temperature and density reach some threshold values, approximately 10^8 K and 10^4 g cm $^{-3}$, respectively. This requires a minimum core mass of $0.33 M_\odot$. Since this mass depends on the initial stellar mass, the luminosity of the star during this phase increases with stellar mass. In intermediate-mass stars (including the lower end of high-mass stars), the core He-burning phase takes place in two regions of the CMD. The first is close to the Hayashi line. Subsequently, when the energy produced in the He core, which is increasing, equals the energy produced in the H shell, which is decreasing, the outer envelope rapidly contracts passing from convective to radiative. Temperature increases and the star migrates to a bluer region. This produces the blue-loop (BL) phase. It appears rather red in Figure 2, as corresponds to the high metallicity of the computed young population.

Both in low- and intermediate-mass stars, a C-O core is formed as a result of core He burning. Upon the exhaustion of He in the core, the mass of the C-O core is constant for low-mass stars, but increases with stellar mass for all the others. The structure of stars is hence formed by a C-O core, a He-burning shell, a H-burning shell, and a H-rich envelope. In low- and intermediate-mass stars, the mass of the C-O core is not high enough to ignite, and an electron-degenerated core again develops. The star expands, produces a convective envelope, and evolves upward, running almost parallel to the RGB. This is the asymptotic giant branch (AGB) phase. Cooling in the regions external to the C-O core extinguishes the H-burning shell, but eventually the expansion of the envelope is stopped by its own cooling, the envelope contracts, and the H shell reignites. This terminates the early-AGB (E-AGB) phase. After that, the He shell becomes thermally unstable. Both the H and He shells alternate as the main sources of energy producing the TP-AGB phase. This process results in efficient mass loss and terminates with the complete ejection of the envelope and the production of a planetary nebula. The remnant is a C-O white dwarf with a mass lower than the Chandrasekhar limit ($1.4 M_{\odot}$). Intermediate- (and low-) mass stars fail to ignite the C-O core.

In high-mass stars, the C-O core ignites in nondegenerate conditions. The fraction of high-mass stars formed in a galaxy is small and their lifetimes short. For these reasons they do not significantly affect the structure of the CMD, and we do not go further in the discussion of their evolution. It is enough to mention that mass loss plays a fundamental role in determining the position in the CMD of core He-burning stars more massive than about $15 M_{\odot}$, and that, after core C-O ignition, they proceed through a series of nuclear burnings and finish their lives in a supernova explosion.

4. MAIN FEATURES OF THE CMD

The main features and the distribution of stars produced by stellar evolution in a CMD can be seen in Figure 2, where a synthetic CMD, computed for constant SFR from 13 Gyr ago to date, is shown. The CMD is based in the Bertelli94 stellar evolution library and the Lejeune et al. (1997) bolometric correction library. The IMF obtained by Kroupa et al. (1993) and a simple CEL with metallicity $Z(t)$ increasing linearly with time, initial value $Z_0 = 0.0001$ and final value $Z_f = 0.02$ have been used. Colors are associated to age intervals to illustrate the distribution of stars in the CMD according to their age. Labels are included to identify the MS, BL, RGB, AGB, HB, and red-clump (RC) phases. The RC is formed by a mix of the reddest HB stars and the bottom part of the core He-burning phase of intermediate-mass stars. The remaining features have been introduced in § 3.

The MS provides the most important and unambiguous age information. But it is interesting to note that, besides it, the BL and the AGB, if well populated, provide useful and complementary age information, which is poor, however, on the RGB. However, the latter gives information on the integrated star formation rate for intermediate and old stellar populations and provides clues to constrain the CEL.

The morphology of the CMD is altered by the presence of binary stars. Figure 3 illustrates the effect, which is most obvious in the lowest MS but also affects the overall distribution of stars in the CMD.

To simplify the discussion of stellar populations based on CMD analysis, it is useful to introduce some terminology. We use the terms *old*, *intermediate-age*, and *young* to specify

three stellar age ranges that are associated to features clearly recognizable in the CMD. By *old* we refer to populations that are not able to produce bright, extended AGBs. This corresponds to ages larger than about 10 Gyr. Good examples of old objects are globular clusters. Old populations will always produce a well-populated RGB and, in addition, they may show a blue extended HB. However, the latter is not a unambiguous age indicator since it depends on metallicity and mass loss on the RGB. *Intermediate-age* populations are those that produce an RGB, as well as extended, bright AGBs. They are older than 1–2 Gyr. Finally, *young* populations are those that ignite He in the nucleus in nondegenerate conditions and therefore fail to produce an RGB. The age separating the young from the intermediate-age ranges is the MS lifetime of stars of mass equal to m_{lw} , the mass separating the low- and intermediate-mass dominions. A pure young population would not have had time for low-mass stars to evolve from the MS.

5. THE CHEMICAL ENRICHMENT LAW OF A STELLAR SYSTEM

In its current version, IAC-STAR offers two main procedures to compute the CEL, $Z(t)$: (1) by linear interpolation in several, arbitrary $Z(t)$ nodes given by the user and (2) from the parameters (yield, infall and outflow rates, etc.) used in physical CEL scenarios. For a better understanding of the second procedure, the CEL fundamentals are outlined in this section. However, it must be kept in mind that IAC-STAR is not a code to solve for CEL scenarios. It allows a wide range of choices for them and computes stars with the necessary coupling between age, metallicity, SFR, and gas fraction provided by the input parameters. But it is the user's responsibility to decide what kind of chemical law is to be used. On the other hand, the linear interpolation in $Z(t)$ nodes, which includes a linear law and a constant one, is a simplistic, perhaps physically unrealistic choice, but it may work well for many users, in particular when details about the actual metallicity law are not known. It must be also noted that a simple, linear CEL is not far from the law of a moderate infall model.

Metallicity laws for a closed box and for infall, outflow of well-mixed material, and outflow of rich material can be found in Peimbert et al. (1994). In IAC-STAR the infall and outflow (of well-mixed material) scenarios can be used as well as the closed-box one, which is but a limiting case of any of the former. The unmixed, rich material outflow can be simulated by the well-mixed material outflow if the yield is allowed to vary, and we are not interested in the helium-to-oxygen ratio, which, in any case, is beyond the scope of this software.

Assuming instantaneous recycling, infall and outflow laws are given by (Peimbert et al. 1994):

$$Z(t) = Z_0 + \frac{y}{\alpha} \{1 - [\alpha - (\alpha - 1)\mu(t)^{-1}]^{-\alpha/(1-\alpha)}\} (\text{Infall}), \quad (1)$$

$$Z(t) = Z_0 + \frac{y}{\lambda + 1} \ln [(\lambda + 1)\mu(t)^{-1} - \lambda] (\text{Outflow}). \quad (2)$$

The chemical enrichment theory has been developed elsewhere (see Tinsley 1980; Peimbert et al. 1994, and references therein), and it is not our aim to discuss it here in any detail. However, the former equations deserve some comment in order to understand the CEL computation in IAC-STAR. The initial metallicity, Z_0 , should be 0 for physically realistic models, but it will be useful to have the possibility of assuming some initial

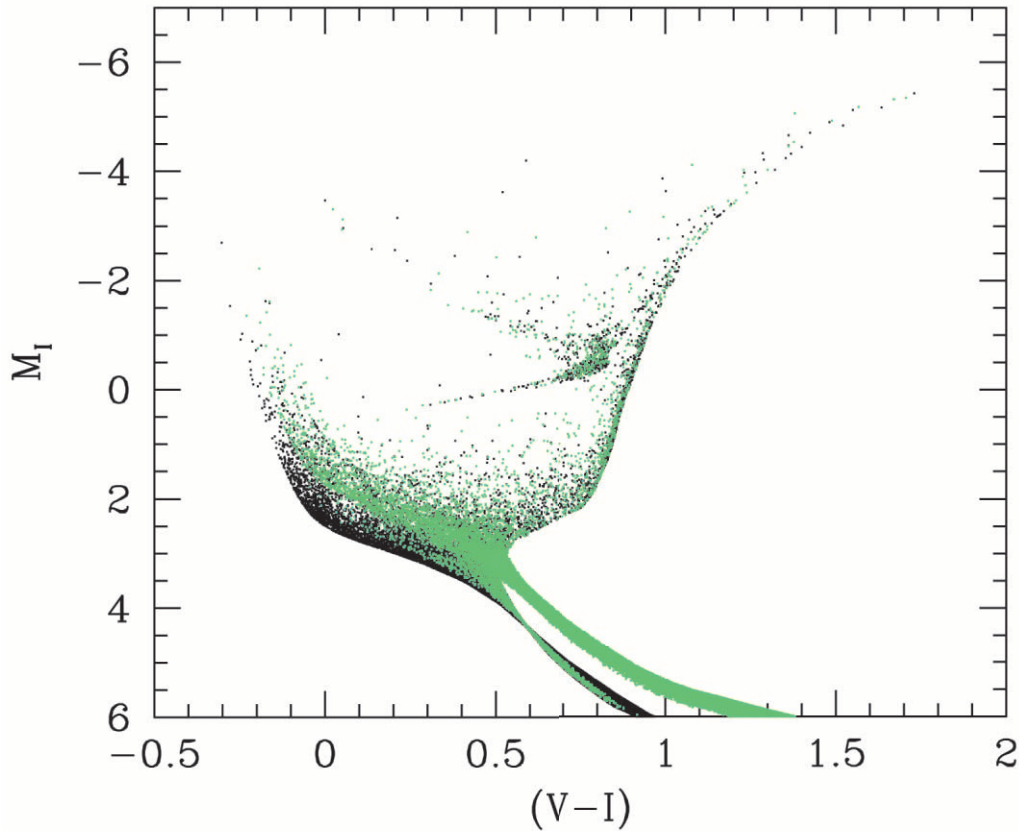


FIG. 3.—Synthetic CMD computed using constant SFR from 13 Gyr ago to date and metallicity linearly increasing from $Z_0 = 0.0001$ to $Z_f = 0.001$, Salpeter IMF, and a 0.3 fraction of binary stars with minimum mass ratio 0.7. The Bertelli94 stellar evolution library and the Lejeune et al. (1997) bolometric correction library have been used. Colors and magnitudes of binary stars are represented in green. Green points in the single-star locus of the MS correspond to binary stars in which the primary is dead.

enrichment in some cases. The yield y is defined as the mass of newly formed metals that a generation of stars ejects to the interstellar medium relative to the mass locked in stars and stellar remnants by the same stellar generation. The value μ is the gas mass fraction relative to the total mass intervening in the chemical evolution, i.e., including stars, stellar remnants, low-mass objects, dust, and the gas itself, but excluding dark matter, which does not intervene in such processes.

Parameters α and λ control infall and outflow, respectively. They are defined as $f_I = \alpha(1 - R)\psi$ and $f_O = \lambda(1 - R)\psi$, where f_I and f_O are the infall and outflow rates, respectively, and R is the mass fraction returned to the interstellar medium by a generation of stars. In this way, $(1 - R)\psi$ is the mass locked into stars and stellar remnants, and f_I and f_O are given as fractions (α and λ) of this mass. A few things must be pointed out. First, since ψ is a function of time, so are f_I and f_O . Second, both α and λ can take values greater than 1. Finally, the simple closed-box model is obtained from any of the former relations if, respectively, $\alpha = 0$ or $\lambda = 0$.

The mass fraction, μ , appearing in equations (1) and (2), is coupled to the SFR, or rather to its integral, by

$$\mu(t) = 1 - \frac{(1 - R)\Psi(t)}{M_0 + (1 - R)\Psi(t)(\alpha - \lambda)}, \quad (3)$$

where M_0 is the initial mass of the system and $\Psi(t) = \int_0^t \psi(t') dt'$. This relation for μ is valid for equations (1) and (2) just using $\lambda = 0$ in the first case and $\alpha = 0$ in the second

one. Let us assume for simplicity, and only in the context of the chemical law computation, that the time unit is the present age of the system, with $t = 0$ for the initial instant and $t = 1$ for the present-day time, and that the integral of the SFR is normalized also for the system age $[\int_0^1 \psi(t') dt' = 1]$. With this, the initial mass of the system can be written as

$$M_0 = (1 - R) \left(\lambda - \alpha - \frac{1}{\mu_f - 1} \right), \quad (4)$$

where μ_f is the final gas fraction. The yield, which is assumed here to be constant, can also be expressed as a function of Z_0 and Z_f (the final metallicity):

$$y = \frac{(Z_f - Z_0)\alpha}{1 - [\alpha - (\alpha - 1)\mu_f^{-1}]^{-\alpha/(1-\alpha)}} \text{ (Infall)}, \quad (5)$$

$$y = \frac{(Z_f - Z_0)(\lambda + 1)}{\ln [(\lambda + 1)\mu_f^{-1} - \lambda]} \text{ (Outflow)}. \quad (6)$$

In practice, the most frequent situation is one in which the researcher has observational information about μ_f and Z_f and can assume that $\mu_0 = 1$ and $Z_0 = 0$ or small. The value of R can be derived from the stellar evolution models (it is $R \simeq 0.2$ for the Padua stellar evolution models, although it depends slightly on the metallicity), and $\psi(t)$ is the key function of the stellar population model (usually what is sought in the analyzed galaxy). The remaining parameters are

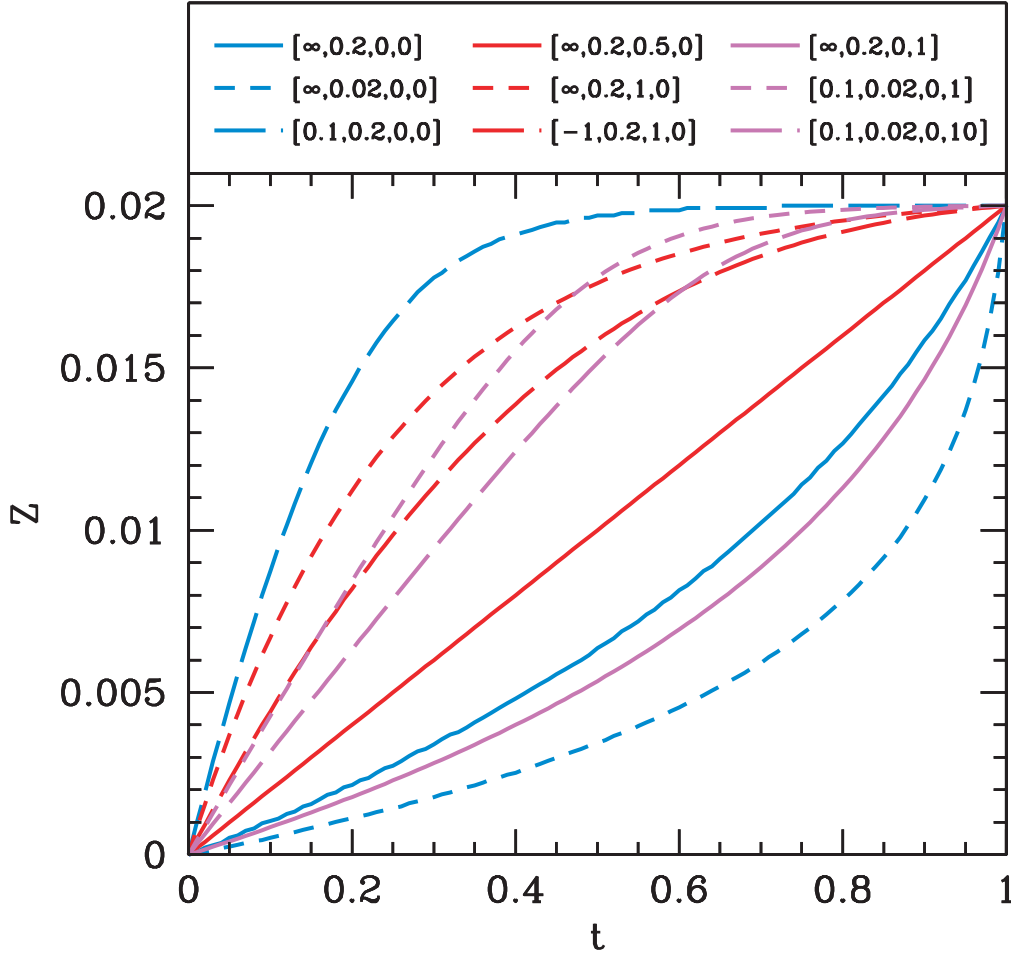


FIG. 4.—Examples of CELs for different choices of μ_f , α , λ , and $\psi(t)$ given for fixed $Z_0 = 0$ and $Z_f = 0.02$. For $\psi(t)$, an exponential law of the form $\psi(t) = A \exp(-t/\beta_\psi)$ has been used, where A is set to normalize the integral of $\psi(t)$ for the entire life of the system. The timescale is normalized, with the instant $t = 0$ corresponding to the beginning of the star formation and the instant $t = 1$ corresponding to its end. In the top panel the parameter choices are displayed. Bracketed figures correspond to $[\beta_\psi, \mu_f, \alpha, \lambda]$. Closed-box models are drawn in blue, infall models in red, and outflow models in magenta.

α and λ , for which reasonable guesses need to be made. Of course, in this way y is no longer the physical stellar yield, but an *effective* yield defined just by equations (5) and (6). If the physical relevance of the chemical evolution model is sought, the consistency of all the parameters must be analyzed. However, for the purposes of computing a synthetic CMD, the chemical law is only an ingredient of the code, which can be imposed from outside. Users of IAC-STAR are encouraged to check and decide the required chemical law. We insist that IAC-STAR only provides the coupling between $\psi(t)$, $\mu(t)$, and $Z(t)$ for the set of input Z_0 , Z_f , μ_f , and α or λ .

In Figure 4 several examples of CELs for different choices of μ_f , α , λ , and $\psi(t)$ are given for fixed Z_0 and Z_f . For $\psi(t)$, an exponential law of the form $\psi(t) = A \exp(-t/\beta_\psi)$ is used. In Figure 5 a law with metallicity dispersion is shown.

6. IAC-STAR COMPUTATION OUTLINE

In this section we outline how the IAC-STAR algorithm works, paying attention to the general interpolation procedure and to how different stellar mass ranges and evolutionary phases are handled. Computation of mass loss in advanced evolutionary phases is explained in the last paragraph. In Figure 1 several tracks of different masses from the Bertelli94 library are plotted as reference for the following discussion.

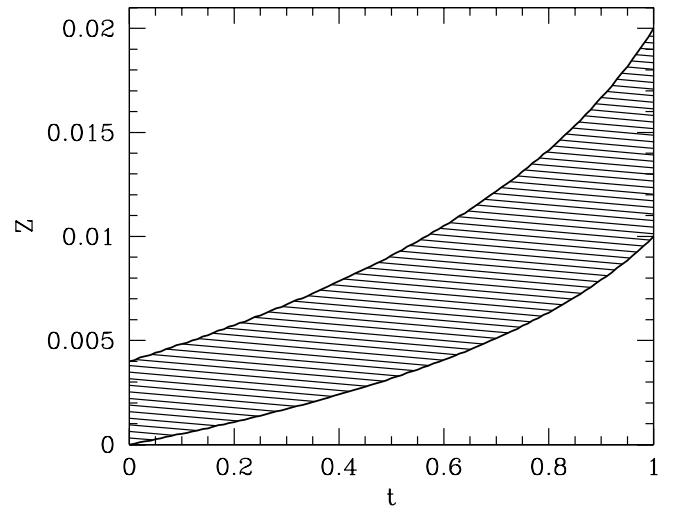


FIG. 5.—Example of a CEL with metallicity dispersion. A constant SFR has been used with $\alpha = \lambda = 0$ and $\mu_f = 0.2$ in both cases, but $Z_0 = 0$, $Z_f = 0.01$ for the lower law and $Z_0 = 0.004$, $Z_f = 0.02$ for the upper one. The timescale is normalized, with the instant $t = 0$ corresponding to the beginning of the star formation and the instant $t = 1$ corresponding to its end. For each age, stars would have metallicities comprised within the shaded area.

6.1. The General Case

As discussed in § 2, a Monte Carlo algorithm and the corresponding probability distribution functions are used to provide the age, a_s , mass, m_s , and metallicity, Z_s , of each synthetic star. In the general, simplest case, mass and metallicity are used to compute the evolutionary track of the star by bi-logarithmic interpolation within the evolutionary track library. It is important to make this simple but important and cumbersome process clear. Note that one of the difficulties is that tracks are not functions, but arbitrary curves, time being the driving parameter. For this, interpolation must be done between homologous sections of different tracks.

Let us first introduce some notation. Tracks are identified by mass and metallicity. We will name tracks by $K_{i,j}$, the first index denoting the metallicity and the second one, the mass. The value Z_s represents a value of metallicity between two values present in the stellar evolution library. The algorithm input does not allow extrapolation outside the library limits in Z . Let us call these two values Z_i^{lib} and Z_{i+1}^{lib} , respectively. So $Z_i^{\text{lib}} \leq Z_s \leq Z_{i+1}^{\text{lib}}$. A search is then made within Z_i^{lib} and Z_{i+1}^{lib} track subsets to look for the mass values embracing m_s . Let us call $m_{i,j}^{\text{lib}}$ and $m_{i,j+1}^{\text{lib}}$ the track mass values embracing m_s for the Z_i^{lib} subset and $m_{i+1,k}^{\text{lib}}$ and $m_{i+1,k+1}^{\text{lib}}$ the same for the Z_{i+1}^{lib} subset. So $m_{i,j}^{\text{lib}} \leq m_s \leq m_{i,j+1}^{\text{lib}}$ and $m_{i+1,k}^{\text{lib}} \leq m_s \leq m_{i+1,k+1}^{\text{lib}}$. The track corresponding to star s can now be obtained by logarithmic interpolation between tracks $K_{i,j}$, $K_{i,j+1}$, $K_{i+1,k}$, and $K_{i+1,k+1}$. Let us call this interpolated track K_s . Additionally, let us call $\tau_{i,j}$ the lifetime of track $K_{i,j}$, i.e., the time at which evolution within that track finish, and τ_s the corresponding lifetime for the interpolated track.

Once K_s has been obtained, the photometric parameters of the star are obtained straightforwardly by logarithmic interpolation of a_s within this track. However, before this it must be established whether the star is dead or alive. This is done by just comparing a_s with τ_s . If $a_s \leq \tau_s$, logarithmic interpolation is performed and the computation is finished for this star. If not, a new dichotomy arises. If the star is of intermediate or high mass, $a_s > \tau_s$ means that it is dead. The mass of the remnant is then computed as explained below and added to the total mass of the system. If the star is of low mass, $a_s > \tau_s$ means that it is beyond the He flash. Computation in the HB track subset must be performed in this case. For this, the mass loss of the star during the RGB is subtracted from m_s (see below) and τ_s is subtracted from a_s . The resulting mass and age, $m_{s,\text{HB}}$ and $a_{s,\text{HB}}$, are used in the HB track subset. Computation is similar to that in the general library. If $a_{s,\text{HB}}$ is larger than the lifetime of the new interpolated HB track, the star is considered dead, and the remnant mass is computed and stored as before.

We have outlined the general computation. However, a few special cases can occur that need more comments. We will treat them in the following.

6.2. Interpolation and Extrapolation between Different Mass Ranges

It may occur that the tracks embracing the mass and metallicity of the synthetic star belong to two different mass ranges (see Fig. 1). If some tracks are in the high-mass range and some in the intermediate-mass range, interpolation can be performed as in the general case up to the end of the tracks. After that, high-mass stars are considered dead, while intermediate-mass stars continue through the TP-AGB, computed as outlined below.

The case is somewhat more complicated if some tracks are in the intermediate-mass range and some in the low-mass range. The stellar physical processes are qualitatively similar for both ranges up to the basis of the RGB: core H-burning (MS) or He-core gravitationally contracting plus shell H-burning (subgiant phase). Interpolation can hence be performed up to that point, but not afterward, when intermediate-mass stars are about to start the core He-burning, while low-mass stars evolve, climbing the RGB. In this case, the mass separating the intermediate- and low-mass ranges is first determined by logarithmic interpolation between the four tracks embracing the mass and metallicity of the synthetic star. This separating mass is used to determine the range to which the star belongs. After this, interpolation is performed up to the RGB basis. Beyond that point, extrapolation is made from tracks of the mass range to which the star belongs. The CMD related features can be seen in Figure 1.

6.3. Very High and Very Low Mass Stars

The stellar mass interval is controlled by the input IMF. Stars of masses beyond the interval covered by the chosen stellar evolution library are handled in different ways depending on the mass being larger than the maximum mass of the library or smaller than the minimum one. In the first case, the star is simply considered dead. The case of very low mass stars is more complex.

The smallest masses computed in the libraries being used are given in Table 1. Stars less massive than that have MS lifetimes larger than the age of globular clusters and are certainly in the MS for any realistic case. They are normally below the limiting magnitude in most CMDs of galaxies. However, they make a quite significant contribution to the total mass of the system, as well as to the integrated luminosity, magnitudes, and colors. Although this contribution can be estimated by integration of the IMF, it may be useful to have the possibility of explicitly computing their colors and magnitudes. For this purpose, the libraries mentioned above have been completed downward in mass using the models by Cassisi et al. (2000). They present MS L and T_{eff} of stars with masses between ~ 0.09 and $0.8 M_{\odot}$ for metallicity values in the range 0.0002 – 0.002 . For present purpose these models have been completed with a very low mass sequence for solar chemical composition (S. Cassisi 2003, private communication). Since these stars have long evolution times and the analysis of the CMD does not usually rely on their exact distribution in it, the effect of age on their L and T_{eff} can be neglected. A polynomial fit has been performed, for each metallicity, to the m - L and the m - T_{eff} plots of the model stars. This can be used to estimate L and T_{eff} of the synthetic star. The coefficients of the fit for the general equation

$$y = a_0 + a_1x + a_2x^2 + a_3x^3 + a_4x^4 + a_5x^5 \quad (7)$$

are given in Table 2. Here, x stands for $\log m$ and y for $\log L$ or $\log T_{\text{eff}}$, respectively.

Figure 1 shows two models computed with these relations for masses 0.4 and $0.6 M_{\odot}$ and $Z = 0.004$. A good agreement exists with the Bertelli94 tracks. Consistency is also quite good in comparisons with the Girardi00 and the Teramo libraries (not shown here). However, the fact that the very low mass stars are computed from a different model set (namely, the one from Cassisi et al. 2000) and that no age computation is made for them must be taken into account if accurate analysis of CMD is intended in the region around $0.6 M_{\odot}$ for

TABLE 2
COEFFICIENTS OF THE $\log L$ – $\log m$ AND $\log T_{\text{eff}}$ – $\log m$ FITS FOR VERY LOW MASS STARS

Relation	a_0	a_1	a_2	a_3	a_4	a_5
$Z = 0.0002, Y = 0.23$:						
$\log L$ vs. $\log m$	1.1387	11.3958	15.8615	8.7825	0.1773	
$\log T_{\text{eff}}$ vs. $\log m$	4.2038	4.3333	13.5738	22.1148	18.2446	6.0709
$Z = 0.0006, Y = 0.23$:						
$\log L$ vs. $\log m$	1.1457	11.7429	16.6033	9.4539	0.3695	
$\log T_{\text{eff}}$ vs. $\log m$	4.1851	4.1282	12.2825	19.1799	15.4070	5.0853
$Z = 0.001, Y = 0.23$:						
$\log L$ vs. $\log m$	1.0342	10.9539	14.2405	6.5840	−0.8234	
$\log T_{\text{eff}}$ vs. $\log m$	4.2229	4.7253	14.9449	24.4181	20.0889	6.6370
$Z = 0.002, Y = 0.23$:						
$\log L$ vs. $\log m$	0.8190	9.6332	10.7591	2.8464	−2.2331	
$\log T_{\text{eff}}$ vs. $\log m$	4.2593	5.4559	18.3152	31.0882	26.0219	8.5882
$Z = 0.02, Y = 0.27$:						
$\log L$ vs. $\log m$	0.3668	9.8685	16.8057	14.4196	3.9769	
$\log T_{\text{eff}}$ vs. $\log m$	3.8133	1.5630	3.2232	2.8249	0.7851	

the Bertelli94 and the Teramo libraries and $0.15 M_{\odot}$ for the Girardi00 library; i.e., around the lower mass limits of these libraries.

6.4. Mass Loss

Mass loss by stellar winds plays an important role in the evolution of massive stars. It is included in the Bertelli94 computation for stars with initial mass larger than $12 M_{\odot}$. The reader is referred to Bertelli94 for details. Besides massive stars, mass loss during the RGB and the AGB has dramatic consequences on the evolution of low- and intermediate-mass stars. In these cases the effects of mass loss are included at the moment of computing synthetic stars in IAC-STAR. Unfortunately, mass loss during these phases and, in particular, during the AGB depends on poorly known physical parameters that should be fine-tuned. In the modeling of mass loss during these phases we follow the criteria given by Bertelli94 and Marigo et al. (1996).

Mass loss during the RGB does not affect the internal structure of the star and can be neglected in the computation of L and T_{eff} . However, the integrated mass loss during this phase determines the mass envelope of the subsequent HB stars and hence its T_{eff} . For this reason, mass loss can be integrated during the RGB and introduced in a single step at the tip of the RGB (TRGB). For this purpose, the empirical relation by Reimers (1975) is used:

$$\dot{m} = 1.27 \times 10^{-5} \eta m^{-1} L^{1.5} T_{\text{eff}}^{-2} M_{\odot} \text{ yr}^{-1}, \quad (8)$$

where L and m are in solar units and η is a scaling parameter. The lowest stellar initial mass for which evolution time up to the TRGB is smaller than or equal to the globular cluster age (about 13 Gyr) is about 0.80 – $0.95 M_{\odot}$, depending on the metallicity, lower masses corresponding to lower metallicities. From this the mass loss during the RGB must be subtracted. Since the core mass at the moment of the He flash is about $0.55 M_{\odot}$, the envelope mass of these stars can be very small. As a consequence, the exact value adopted for η strongly affects T_{eff} at the zero-age HB. In the current version of IAC-STAR, η has a default value of 0.35, but it can be modified by the user.

Computing the mass loss during the AGB is more complicated. It can be neglected during the E-AGB, but it is the key parameter controlling the final evolution of the star during

the TP-AGB. Stellar evolution models of low- and intermediate-mass stars are in general computed up to the beginning of the TP-AGB only. From that point on, computation is performed within IAC-STAR following the prescriptions by Marigo et al. (1996). First, the starting point of the TP-AGB is assumed to be the point in the track just before the first significant He-shell flash. Hence, the evolution through the TP-AGB is followed using several basic relations: (1) the mass loss rate, (2) a relation connecting the core mass with the total luminosity of the star, (3) the rate at which the core mass increases as a result of shell H-burning, and (4) an L – T_{eff} relation for the TP-AGB. Details on these relations can be found in Marigo et al. (1996) and references therein. We briefly summarize them here for consistency.

The mass-loss rate is taken as the minimum of the two following values:

$$\log \dot{m} = -11.4 + 0.0123P, \quad (9)$$

$$\dot{m} = 6.07023 \times 10^{-3} L c^{-1} v_{\text{exp}}^{-1}, \quad (10)$$

where m and L are the stellar mass and luminosity (in solar units), P is the pulsation period (in days), c is the light speed (in kilometers per second) and v_{exp} is the terminal velocity of the stellar wind (in kilometers per second). Equations (9) and (10) stand for periods shorter and larger than about 500 days, respectively. The wind expansion velocity is calculated in terms of the period as (Vassiliadis & Wood 1993):

$$v_{\text{exp}} = -13.5 + 0.056P, \quad (11)$$

and the period is derived from the period-mass-radius relation by Vassiliadis & Wood (1993):

$$\log P = -2.07 + 1.94 \log R_* - 0.9 \log m, \quad (12)$$

where R_* is the stellar radius in solar units.

To connect the core mass with the total luminosity of the star, the following two equations are used:

$$L = 238,000 \mu_w^3 Z_{\text{CNO}}^{0.04} (m_c^2 - 0.0305 m_c - 0.1802) \quad (13)$$

for stars with core mass in the range $0.5 \leq m_c \leq 0.66$ (Boothroyd & Sackmann 1988), and

$$L = 122,585 \mu_w^2 (m_c - 0.46) m^{0.19} \quad (14)$$

for stars with $0.95 \leq m_c$ (Iben & Truran 1978; Groenewegen & de Jong 1993). For stars in the interval $0.66 < m_c < 0.95$, linear interpolation is performed. In the former equations, Z_{CNO} is the total abundance (in mass fraction) of carbon, nitrogen, and oxygen in the envelope, and $\mu_w = 4/(5X + 3 - Z)$ is the average molecular weight for a fully ionized gas, where X and Z are the hydrogen and metal abundances, respectively.

The rate at which the core mass increases as a result of shell H burning is computed using

$$\frac{\partial m_c}{\partial t} = 9.555 \times 10^{-12} \frac{L_H}{X}, \quad (15)$$

where X is the hydrogen abundance (in mass fraction) in the envelope and L_H is the luminosity produced by the H-burning shell (in solar units). In fact, the latter is computed by the relation (Iben 1977):

$$L = L_H + 2000(M/7)^{0.4} \exp[3.45(m_c - 0.96)]. \quad (16)$$

Finally, the L - T_{eff} relation of the TP-AGB is obtained by extrapolating the slope of the E-AGB. In fact, to minimize random effects and possible inconsistencies, the slope is computed using the following relation, obtained by bilogarithmic fit of the slopes of all the models at the end of the E-AGB:

$$\log\left(-\frac{\partial L}{\partial T_{\text{eff}}}\right) = -2.870 + 0.994 \log L - 0.110 \log Z, \quad (17)$$

where Z is the metallicity.

Using the former relations, the TP-AGB is computed for each HB and intermediate-age evolutionary track with mass $m \leq 5 M_{\odot}$, according to the intermediate-mass limit found by Marigo et al. (1996). The TP-AGB computation is terminated either when the envelope mass is zero or the core mass reaches the Chandrasekhar limit ($1.4 M_{\odot}$).

7. RUNNING IAC-STAR

IAC-STAR is made available for free use.² A number of interactive software facilities are intended to be made available from this site, together with IAC-STAR itself. In fact, the content and format of the page is expected to be updated, including new software and taking into account user feedback. In the present form, a template is provided in which several input parameters can be entered. For all them, default values, as well as a brief option list for quick reference, are available. Once all the inputs are provided, the user can request that the program be executed. This is performed by a dedicated computer at the Instituto de Astrofísica de Canarias (IAC). The resulting data file is stored upon completion in a public-access ftp directory at the IAC. The address of this directory is given to the user by email, to the address provided by him- or herself, together with the output file name and information on the inputs used and the output file content. In the following we describe the input parameters and the output file content. Since

the specific content of both may change in future versions of the software, only a general description of them is provided. Detailed, updated information can be found in the IAC-STAR Web site.

7.1. Input Parameters

The input parameters are introduced as follows (see the IAC-STAR Web site for updated details):

1. The chosen stellar evolution and bolometric correction libraries.
2. A seed for the random number generator. The routine used for random number generation is “ran2,” obtained from Numerical Recipes in Fortran (Press et al. 1997).
3. Total number of stars computed or saved into the output file. To prevent excessively long runs, the maximum allowed total computed and saved stars are limited to some big numbers.
4. The minimum stellar luminosity or maximum magnitude in a given filter. Although fainter stars are computed, only those brighter than this value are saved into the output file.
5. The SFR, $\psi(t)$. It is computed by interpolation between several $\psi(t)$ nodes, defined by the user arbitrarily, or using an analytical function of the form $\psi(t) = \exp(-t/\beta_{\psi})$.
6. The chemical enrichment law. Two alternative approaches are allowed to produce the chemical enrichment law: (a) just an interpolation between several time-metallicity nodes, defined by the user and permitting a completely arbitrary metallicity law; (b) computation from usual parameters involved in physical scenarios of chemical evolution, even though a self-consistent physical formulation is not intended in this case. Metallicity dispersion is allowed in both cases.
7. The IMF. It is assumed to be a power law of the mass, but several mass intervals can be defined.
8. Binary star control. Both the fraction of binary stars and the secondary to primary minimum mass ratio can be supplied.
9. Mass-loss parameter. Although the default $\eta = 0.35$ seems a reasonable choice, the user can modify it here. It must be noted that η significantly affects the extension of the HB for low-metallicity stars.

7.2. The Output File Content

In the current version, the content of the output file is organized as follows (see the IAC-STAR Web site for updated details):³

1. A header containing information about the input parameters. This includes in particular the libraries used, the total number of computed and stored stars, the minimum luminosity or maximum magnitude stored, the current SFR, CEL, and IMF laws, the fraction of binaries and minimum secondary-to-primary mass ratio, and a heading line for the column content, including a list of the photometric bands for which magnitudes have been computed.
2. Several lines each containing the information for a single or binary star. This information includes physical parameters (luminosity, temperature, gravity, mass, and metallicity), photometric parameters, and age.
3. Closing lines. Integrated quantities are provided in the file closing lines, including the total number of stars ever formed, currently alive, and stored; the total mass ever incorporated into stars [in other words, just the time integral of the

² Available at <http://iac-star.iac.es>.

³ At <http://iac-star.iac.es>.

SFR, $\int_0^T \psi(t) dt$]; the mass currently locked into living stars and into stellar remnants, and the total luminosity and the integrated magnitudes. Besides these integrated quantities, the logarithm of the sum of squared luminosities ($\log \sum_i L_i^2$, where L_i is the luminosity of the i th star if it is single or the total luminosity of the system if it is binary), and the magnitudes derived from this are also given. These are the magnitudes associated to surface brightness fluctuations (SBFs). In this sense, IAC-STAR can be used as a SBF population synthesis code (see Marín-Franch & Aparicio 2004).

8. FINAL REMARKS AND CONCLUSIONS

The program IAC-STAR, designed to generate synthetic CMDs, is presented in this paper. It calculates full synthetic stellar populations on a star-by-star basis, by computing the luminosity, effective temperature, and magnitudes of each star. A variety of stellar evolution and bolometric correction libraries, SFRs, IMFs, and CELs are allowed, and binary stars can be computed. The program provides also integrated masses, luminosities, and magnitudes, as well as SBF luminosity and magnitudes for the total synthetic stellar population. In this way, although it is mainly intended for synthetic CMD computation, it can be also used for traditional and SBF population synthesis research.

Among the main characteristics of the program, the following are the most relevant:

1. Luminosity and effective temperatures of each star are computed by direct bilogarithmic interpolation in the age-metallicity grid of a stellar evolution library. Two Padua libraries (Bertelli94 and Girardi00) and the new Teramo library (Pietrinferni et al. 2004) are used in the current version completed by the Cassisi et al. (2000) models for very low mass stars. This produces a smooth distribution of stars in the output

synthetic CMD, which is necessary if accurate studies of SFH are intended.

2. Mass loss is computed during the RGB and the AGB phases.

3. The AGB phase is extended to the TP-AGB, in this way covering all the significant stellar evolution phases accurately.

4. Color and luminosities in a variety of visual broadband, infrared, and *HST* filters are provided. Bolometric correction transformations by Girardi et al. (2002), Castelli & Kurucz (2003), Fluks et al. (1994), Lejeune et al. (1997), and Origlia & Leitherer (2000) are used for this purpose.

The program is offered for free use and can be executed at the site <http://iac-star.iac.es>, with the single requirement that this paper be referenced and the IAC acknowledged in any derived publication. Our intention is to produce further improved versions of the program following feedback by the user community.

We are deeply indebted to Cesare Chiosi, Gianpaolo Bertelli, and other colleagues of the Padua stellar evolution group for a fruitful, long-term collaboration. Building up IAC-STAR would not have been possible without this collaboration. We are also indebted to Santi Cassisi for his help in the implementation of the Teramo stellar evolution library and corresponding bolometric corrections, and for many useful discussions and advice. The Computer Division of the IAC is acknowledged for implementing the hardware and the Web site interface of the program. Financial support has been provided by the IAC Research Division. The authors are funded by the IAC (grant P3/94) and by the Science and Technology Ministry of Spain (grant AYA2001-1661 and AYA2002-01939).

REFERENCES

- Alexander, D. R., & Ferguson, J. W. 1994, *ApJ*, 437, 879
 Angulo, C., et al. (NACRE Collaboration). 1999, *Nucl. Phys. A*, 656, 3
 Aparicio, A. 2002, in *ASP Conf. Ser. 274, Observed H-R Diagrams and Stellar Evolution Models*, ed. T. Lejeune & J. Fernandes (San Francisco: ASP), 429
 Aparicio, A., Gallart, C., & Bertelli, G. 1997a, *AJ*, 114, 669
 ———. 1997b, *AJ*, 114, 680
 Aparicio, A., Gallart, C., Chiosi, C., & Bertelli, G. 1996, *ApJ*, 469, L97
 Aparicio, A., & Hidalgo, S. 2004, in preparation
 Aparicio, A., Tikhonov, N., & Karachentsev, I. 2000, *AJ*, 119, 177
 Ardeberg, A., Gustafsson, B., Linde, P., & Nissen, P. E. 1997, *A&A*, 322, L13
 Bertelli, G., Bressan, A., Chiosi, C., Fagotto, F., & Nasi, E. 1994, *A&AS*, 106, 275 (Bertelli94)
 Bertelli, G., Mateo, M., Chiosi, C., & Bressan, A. 1992, *ApJ*, 388, 400
 Bertelli, G., & Nasi, E. 2001, *AJ*, 121, 1013
 Bertelli, G., Nasi, E., Girardi, L., Chiosi, C., Zoccali, M., & Gallart, C. 2003, *AJ*, 125, 770
 Bressan, A. G., Chiosi, C., & Bertelli, G. 1981, *A&A*, 102, 25
 Boothroyd, A. I., & Sackmann, I.-J. 1988, *ApJ*, 328, 641
 Cassisi, S., Castellani, V., Ciarcelluti, P., Piotto, G., & Zoccali, M. 2000, *MNRAS*, 315, 679
 Castelli, F., Gratton, R. G., & Kurucz, R. L. 1997, *A&A*, 318, 841
 Castelli, F., & Kurucz, R. L. 2003, *Poster A20 IAU Symp. 210, Modeling of Stellar Atmospheres*, ed. N. E. Piskunov et al. (San Francisco: ASP)
 Caughlan, G. R., & Fowler, W. A. 1988, *At. Data Nucl. Data Tables*, 40, 283
 Chiosi, C. 1998, in *Stellar Astrophysics for the Local Group*, ed. A. Aparicio, A. Herrero, & F. Sánchez (Cambridge: Cambridge Univ. Press), 1
 Chiosi, C., Bertelli, G., & Bressan, A. 1988, *A&A*, 196, 84
 ———. 1992, *ARA&A*, 30, 235
 Cox, A. N., & Stewart, J. N. 1970a, *ApJS*, 19, 243
 ———. 1970b, *ApJS*, 19, 261
 Dohm-Plamer, R. C., et al. 1997, *AJ*, 114, 2527
 Dolphin, A. E. 1997, *NewA*, 2, 397
 Fluks, M. A., et al. 1994, *A&AS*, 105, 311
 Gallart, C., Aparicio, A., Bertelli, G., & Chiosi, C. 1996, *AJ*, 112, 1950
 Gallart, C., Freedman, W. L., Aparicio, A., Bertelli, G., & Chiosi, C. 1999, *AJ*, 118, 2245
 Girardi, L., Bertelli, G., Bressan, A., Chiosi, C., Groenewegen, M. A. T., Marigo, P., Salasnich, B., & Weiss, A. 2002, *A&A*, 391, 195
 Girardi, L., Bressan, A., Bertelli, G., & Chiosi, C. 2000, *A&AS*, 141, 371 (Girardi00)
 Girardi, L., Bressan, A., Chiosi, C., Bertelli, G., & Nasi, E. 1996, *A&AS*, 117, 113
 Groenewegen, M. A. T., & de Jong, T. 1993, *A&A*, 267, 410
 Harris, J., & Zaritsky, D. 2001, *ApJS*, 136, 25
 Hernández, X., Valls-Gabaud, D., & Gilmore, G. 1999, *MNRAS*, 304, 705
 Holtzman, J. A., et al. 1999, *AJ*, 118, 2262
 Huebner, W. F., Merts, A. L., Magee, N. H., & Argo, M. F. 1997, Los Alamos Sci. Lab. Rep. LA-6760-M (Los Alamos: Los Alamos Opacity Library)
 Hurley-Keller, D., Mateo, M., & Nemec, J. 1998, *AJ*, 115, 1840
 Iben, I. 1977, *ApJ*, 217, 788
 Iben, I., & Truran, J. W. 1978, *ApJ*, 220, 980
 Iglesias, C. A., & Rogers, F. J. 1996, *ApJ*, 464, 943
 Irwin, A. W., et al. 2004, in preparation
 Kippenhahn, R., Thomas, H.-C., & Weigert, A. 1965, *Z. Astrophys.*, 61, 241
 Kroupa, P., Tout, C. A., & Gilmore, G. 1993, *MNRAS*, 262, 545
 Kunz, R., Fey, M., Jaeger, M., Mayer, A., Hammer, J. W., Staudt, G., Harissopulos, S., & Paradellis, T. 2002, *ApJ*, 567, 643
 Kurucz, R. L. 1992, in *Stellar Populations of Galaxies*, ed. B. Barbuy & A. Renzini (Dordrecht: Kluwer), 225
 Landré, V., Prantzos, N., Aguer, P., Bogaert, G., Lefebvre, A., & Thibaud, J. P. 1990, *A&A*, 240, 85
 Lejeune, T., Cuisinier, F., & Buser, R. 1997, *A&AS*, 125, 229
 Maeder, A. 1974, *A&A*, 32, 177
 Marigo, P., Bressan, A., & Chiosi, C. 1996, *A&A*, 313, 545
 Marín-Franch, A., & Aparicio, A. 2004, in preparation
 Mihalas, D., Hummer, D. G., Mihalas, B. W., & Däppen, W. 1990, *ApJ*, 350, 300

- Ng, Y. K., Brogt, E., Chiosi, C., & Bertelli, G. 2002, *A&A*, 392, 1129
- Origlia, L., & Leitherer, C. 2000, *AJ*, 119, 2018
- Peimbert, M., Colín, P., & Sarmiento, A. 1994, in *Violent Star Formation: from 30 Doradus to QSOs*, ed. G. Tenorio-Tagle (Cambridge: Cambridge Univ. Press)
- Pietrinferni, A., Cassisi, S., Salaris, M., & Castelli, F. 2004, *ApJ*, submitted
- Press, W. H., Teukolsky, S. A., Vetterling, W. T., & Flannery, B. P. 1997, *Numerical Recipes in FORTRAN 77* (Cambridge: Cambridge Univ. Press)
- Reimers, D. 1975, *Mem. Soc. R. Sci. Liege*, 8, 369
- Rogers, F. J., & Iglesias, C. A. 1992, *ApJS*, 79, 507
- Stappers, B. W., et al. 1997, *PASP*, 109, 292
- Tinsley, B. 1980, *Fund. Cosmic Phys.*, 5, 287
- Tolstoy, E., & Saha, A. 1996, *ApJ*, 462, 672
- Tosi, M., Greggio, L., Marconi, G., & Focardi, P. 1991, *AJ*, 102, 951
- Vallenari, A., Bertelli, G., & Schmidtobreick, L. 2000, *A&A*, 361, 73
- Vallenari, A., Chiosi, C., Bertelli, G., Aparicio, A., & Ortolani, S. 1996a, *A&A*, 309, 367
- Vallenari, A., Chiosi, C., Bertelli, G., & Ortolani, S. 1996b, *A&A*, 309, 358
- Vassiliadis, E., & Wood, P. R. 1993, *ApJ*, 413, 641
- Weaver, T. A., & Woosley, S. E. 1993, *Phys. Rep.* 227, 65